Published by :
http://www.ijert.org

International Journal of Engineering Research & Technology (IJERT)
ISSN: 2278-0181
Vol. 5 Issue 02, February-2016

Biosorbent for Diazo Acid Dye Removal as a Contribution to Textile Wastewater Treatment

F. Ayari and M. Trabelsi Ayadi
Laboratoire des **A**pplications de la **C**himie aux **R**essources et **S**ubstances **N**aturelles **e**t a` l'**E**nvironnement (**LACReSNE**),
Université de Carthage, Faculté de Sciences de Bizerte, Zarzouna 7021, Tunisia.

Abstract:- **Adsorption of Congo red (CR) from water solution through batch adsorption experiments onto locally bentonite befor and after modification by using hexadecyltrimethylammonium (HDTMA) bromide at 3 CEC level, obtained organosmectie labeled ArPM was characterized by several methods such as X-ray diffraction (XRD), Infrared spectroscopy (IR), thermal analysis (TGA-DTG), Brunauer-Emmett-Teller (BET) and SEM, these methods were used to provide new visions into the interlayer structure of the synthesized hybrid organoclay. XRD patterns showed the changes in the d(001) spacing, which gave details of the arrangement of surfactant in the organoclays, IR spectroscopy showed the existence of HDTMA functional groups on bentonite surface. The BET surface area significantly decreased after the modification due to the coverage of the pores of purified smectite. Acid-base potentiometric titration and zeta metric behavior of the smectite before and after organophilisation were investigated. Smectite surface which was hydrophilic in nature convert to hydrophobic after organophilisation. Hybrid material develops more positives surface charges and great basal spacing layer; therefore these materials can be very useful to remove anionic pollutants from wastewater.**

After the characterization, the adsorption of a textile diazo acid dye, Congo red (CR), onto smectite and HDTMA-smectite was investigated. The maximum adsorption capacity of smectite and HDTMA-smectite for CR was remarkable at 20°C.

Isotherm data were investigated according to Langmuir and Freundlich equations. Monolayer adsorption can be estimated for CR removal by the smectite sorbent.

Keywords-Smectite, Adsorption; Acid textile dye; Sorption isotherms; Langmuir and Freundlich models.

1. INTRODUCTION

The problems of the environment constituted an integral part of the development strategies conceived and implemented in each country at the national level as a sector level. The industry of dyes generates rejections, pollutants, toxic heterogeneous composition, which became a source of watery pollution. It is a real degradation of environment; it is an enormous harmful effect for human health. Textile dyes present a very weak biodegrability [1] what makes the biological treatments difficult and in case of degradation, they may produce carcinogenic substances. Several processes of elimination were used; such as adsorption on activated carbon which is an effective process but expensive and produces a mud which constitutes itself an environmental threat. Therefore there has been increasing interest in research into cheaper and more readily available adsorbents. Some biological adsorbents have also been studied for the adsorption of reactive dyes; these include amongst others; apple pomace and wheat straw, corncob and barley husk, maize cob, wood and rice husk. These adsorbents were found to be efficient in binding with basic dyes rather than acid dyes. Research acted towards processes of treatment using natural materials. In recent years attention has been focalized in clay mineral due to its abundant availability, also according to its important surface and presence of loads on its surface and interlayers space, which gives it, the possibility of exchanging. However, most previous works are based on modification of these adsorbents via physical and chemical process, which is necessary for the adsorption of anionic dyes, as the net negative charge on the dye and clay surface brings charge repulsion and thus, resulting in lowering surface interaction and adsorption.

A study effected on chemical classifications of dyes, shows that diazo dyes are the most toxic [2].Toxicity by exposure to the azo dyes and their metabolites is not a new fact. Since 1895, the increase in the number of cancers of bladder observed in workmen of textile industry is connected to their exposure prolonged to the azo dyes [3].
The adsorption of organic cationic dyes by clay minerals has been investigated for many years. There is very little information on the adsorption of organic anions by clay minerals in the literature. Also, there are contradictory results about the effect of pH on the adsorption of CR by various adsorbents in the literature. In this study we report the ability of locally clay mineral before and after modification to remove diazo acid dye (CR) from aqueous solution as a contribution to anionic dye removal from textile wastewaters. The clay sample collected demonstrates a good affinity with this anionic dye.

II. MATERIALS AND METHODS

II .1 Materials

Congo Red (CR) is a synthetic anionic secondary diazo dye, belonging to the family of reactive dyes which contain chromophoric groups.The molecular weight of CR is 696,66 g.mol^{-1}, the maximum wavelength absorption in the field of visible is λ_{max} = 497 nm. The IUPAC name of CR is [1-napthalene sulfonic acid, 3,3 -(4,4 –biphenylene bis (azo))bis (4-amino-) disodium salt], its structural formula is: $C_{32}H_{22}N_6Na_2O_6S_2$.

Congo red contains $–NH_2$ and $–SO_3$ functional groups (fig1). The CR sodium saltis responsible for dying cotton full red and is the first synthetic dye capable of directly dying cotton [4]. It has a strong affinity for

(This work is licensed under a Creative Commons Attribution 4.0 International License.)

International Journal of Engineering Research & Technology (IJERT)
ISSN: 2278-0181
Vol. 5 Issue 02, February-2016

cellulose fibers, very used in textile industry. Congo Red was used without any further purification.
The color of CR changes from red to blue in the presence of inorganic acids. The change of color is due to the resonance between charged canonical structures [5]. The red color is stable in the pH range of 5–10 [6]. The stock solution of CR was prepared by dissolving known quantity of CR powder in distilled water, successive dilutions were made to obtain the working solution at desired concentrations.

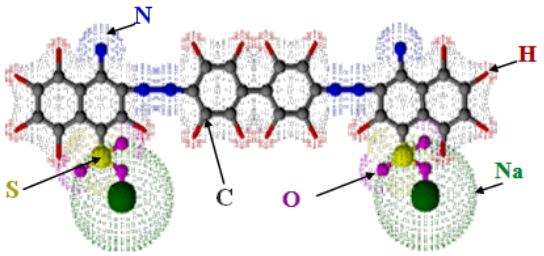

fig. 1 Chemical structure of Congored

Clay, used in this study, is a naturally calcium smectite.
For purified clay, raw clay was previously crushed and sieved, then suspended in polyethylene bottle containing a solution of NaCl (1 M). After 12 hours of agitation, the clay particles are separated from the stage water by centrifugation at a speed of 6000 rpm for 30 min $^{-1}$. This step is repeated several times to provide near complete substitution of the interlayer ions (Ca^{2+}, Mg^{2+}, Li^{+}…) by sodium ion and finally obtain purified Na saturated clay. Impurities such as carbonate, quartz, calcite etc...associated to the clay fraction are also eliminated.
The Na saturated (ArP) clay is finally washed with distilled water several times; this step is followed by a dialysis process to remove the excess of chloride ions, $AgNO_3$ test is needed to verify the elimination of chloride ions. Obtained clay is collected in a Teflon beaker, dried at 333K and then crushed and sieved.

Organoclays

surfactant-modified smectite (ArPM) was prepared by mixing an amount of Na-smectite, initially dispersed in ~100 mL of deionized water, with a stoichiometric amount of surfactant (tree time the cation of exchangeable cation of ArP (3CEC)) dispersed in 200mL of deionized water, added slowly to the clay suspension, Surfactant used in this study is precisely hexadecyltrimethylammonium bromide (fig.2). The reaction mixtures were stirred for 12 h at 80ºC. After maturation, centrifugation, and several successive dialyses, the prepared organoclay materials was washed with distilled water to remove any excess surfactants, until free of bromide anions (tested by $AgNO_3$), dried at 80 ºC, ground in an agate mortar and passed through a 200 mesh sieve. The organoclay prepared was marked as H_3-bent.

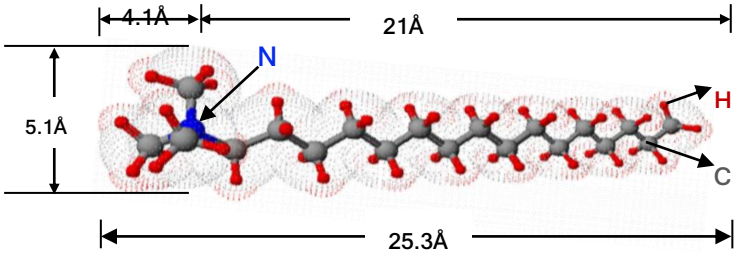

fig.2: Chemical structure of HDTMA

II.2. Methods

Composition of the clay sample was identified by X-ray diffractometer (XRD). XRD analysis was carried out using a PANalytical X'Pert High Score Plus diffractometer, CuKα radiation. Composition of ArP sample was confirmed with an EDX system. The Fourier transform infrared (FTIR) spectra were acquired on a Perkin Elmer 783 dispersive spectrometer in the range of 4000–400 cm^{-1}. Cation exchange capacities (CEC) was estimated as described in previous studies [7,8]. As complimentary technicals for clay characterization, the sample morphology was recognized by Transmission electron microscopy (TEM). BET surface area (S_{BET}) and pore volumes of adsorbent were measured using the physical adsorption of nitrogen by Quantachrome Autosorb-1 instrument. Zeta potential measurement using a Zetasizer 3000 HSA (Malvern Instruments) and potentiometric titration at different ionic strength were used to estimate the points of zero proton charge of used adsorbents. Uv-spectrometer was also used to determine the percent of dye removal by ArP and ArPM under several conditions such as pH, dye concentration…

III. RESULTS AND DISCUSSIONS

III.1 Characterization of the adsorbents

(This work is licensed under a Creative Commons Attribution 4.0 International License.)

International Journal of Engineering Research & Technology (IJERT)
ISSN: 2278-0181
Vol. 5 Issue 02, February-2016

III.1.1 Chemical analyzes

Purified clay was performed by means of X-ray fluorescence spectrometer (Table 1).Chemical composition is given in weight percent of oxides.

Results stipulate the presence of silica and alumina as major constituents along with traces of potassium, magnesium and calcium oxides [9].

Table 1: Chemical composition (%weight (w%)) of Sodium smectite ArP

MxOy	SiO_2	MgO	CaO	Fe_2O_3	Al_2O_3	Na_2O	K_2O
%weight	52	4.2	0.4	4.8	15.56	1.63	0.76

Accordingly the average structural formula of the Na exchanged purified clay is:

$Ca_{0.05}Na_{0.145}K_{0.479}(Si_{7.87}Al_{0.13})(Al_{2.6}Fe_{0.678}Mg_{0.547})O_{22}$

The formula shows that the two types of substitutions exist (octahedral and tetrahedral substitutions) which gives a beidellitic–montmorillonitic character to this smectite.

III.1.2 X-Ray diffraction

The clay sample, before and after purification, analyzed by XRD measurements (fig.3 and fig.4) showed that clay is composed mainly of smectite, kaolinite, illite, and quartz. The smectite is deduced by the appearance of peaks at 15.3Å on the normal diffractogram of the raw sample ArB) which was displaced to 12.38 Å after purification and which was enlarged on the glycoled diffractogram to 17.69 Å. The presence of kaolinite is proved by the appearance of peaks at 7.19 and 3.57 Å on the normal and glycoled diffractograms. These peaks disappear in the sample heated at 550°C during 2 h. The appearance of peaks at 4.27and 3.35Å marked the presence of quartz, witch disappears after purification, and peaks at 10.32 and 2.57 Å marked the presence of illite [10, 11]. Heating the sample above 550°C collapses the interlayer spacing at 10Å, this data support the clays mectite group.

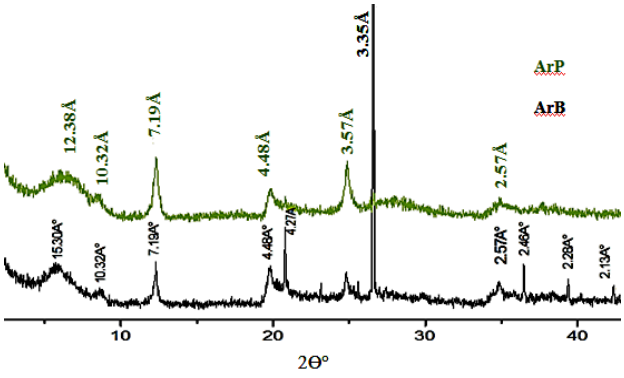

fig.3: X-raydiffractogram of samples ArB and ArP

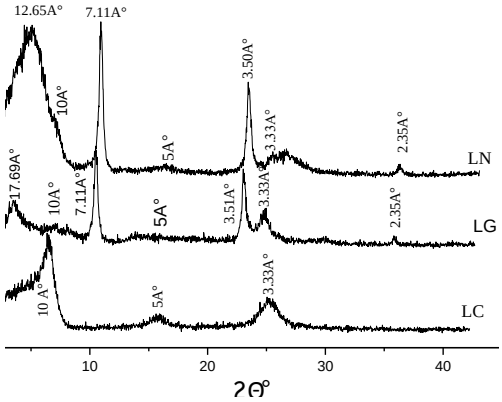

fig 4: diffractogram of oriented samples of ArP (LC: heated blade, LG glycol blade; LN: normal blade)

III.1.3 FTIR analysis

The infrared spectra were recorded with Perkin Elmer 783 dispersion spectrometer in the range of 4000 to 400 cm^{-1}. Spectra were obtained by accumulating 128 scans at a resolution of 4 cm^{-1}. FTIR spectroscopy has been employed to pinpoint the most significant modification by means of HDTMA grafting in the purified smectite (ArP). Therefore spectrum of ArP, surfactant molecule, and synthesized HDTMA modified smectite (organoclay sample ArPM) (fig. 5) were carried out and compared with each other to obtain information regarding modification of smectite with HDTMA functional groups.

As can be seen from figure 5 and on the basis of information given by earlier works [12-13] absorption bands at 3626cm^{-1} and 3622 in ArP and ArPM respectively are owing to hydroxyl group vibration in Mg-OH-Al, Al-OH-Al and Fe-OH-Al elements of the octahedral layer.

Position and shape of the –OH stretching band in the FT-IR spectra of smectite mineral is basically influenced by the nature of the octahedral atoms to which the hydroxyl groups are coordinated. Thus absorption band at 3626 cm^{-1}, found in the spectrum of ArP, is typical for smectite with large amounts of Al in the octahedral sheet.

Broad band's at around 3430 in both ArP and ArPM were attributed to H–O–H stretching vibration of adsorbed water. Appearance of intense peak at around 3017 cm^{-1} (stretching peak of the N-H groups) in the infrared spectrum of ArPM is a suggestion of interaction between smectite structure and functional groups of surfactant.

Peaks at around 1623 and 1648 cm^{-1} relate to the OH^- deformation of water (H-O-H bending), reveals the presence of adsorbed water. These bands appear in both ArP (1623cm^{-1}) and ArPM (1648 cm^{-1}) [14], yet it's position shifted from 1623 cm^{-1} to 1649cm^{-1} witch reflects that the amount of hydrogen bonded water molecules present in the organoclay is less than those with ArP. This could be explained by that the H_2O content is reduced with the replacement of the hydrated cations in the interlayer space of smectite by $HDTMA^+$ ions. Therefore internal surface property of smectite was converted from hydrophilic to hydrophobic. In addition, comparing to HDTMA spectra, infrared spectrum of organoclay showed a pair of a strong intense vibrations at around 2921 and

(This work is licensed under a Creative Commons Attribution 4.0 International License.)

International Journal of Engineering Research & Technology (IJERT)
ISSN: 2278-0181
Vol. 5 Issue 02, February-2016

2854 cm^{-1} attributed to symmetric and asymmetric stretching vibrations of methylene groups (ν_{CH2}), which are absent in ArP, this attest transformation of purified smectite on organoclay with the surfactant cation ($HDTMA^+$). These frequencies are extremely sensitive to the conformational ordering of the chain of cationic surfactant onto clay [15], in this case vibration bands close to micelle surfactant configuration as reported by Xi in a previous studies [16].

Existence of peak at around 1473 cm^{-1} in ArPM spectrum (which is absent in ArP), specifying the presence of C-N vibrations of tertiary amines. The spectrum was similar to those of solid HDTMA because the chains were densely packed; this observation clearly indicates that the surface modification of ArP is achieved by surfactant.

Adsorption band at around 720cm^{-1} correspond to the methylene rocking mode, independent of chain conformation, this mode is split due to interchain interaction between contiguous CH_2 groups of adjoining chains [15].

The bands at around 1110 and 1030 $cm^{-1,}$ represent the Si–O coordination vibrations and the stretching of Si–O in the Si–O–Si groups of the tetrahedral sheet, respectively. Also, Si–O–Al (octahedral) and Si–O–Si bending vibrations were observed at 520 and 470 cm^{-1}, respectively, for both ArP and organo-smectite, as in other silica and silicate systems.

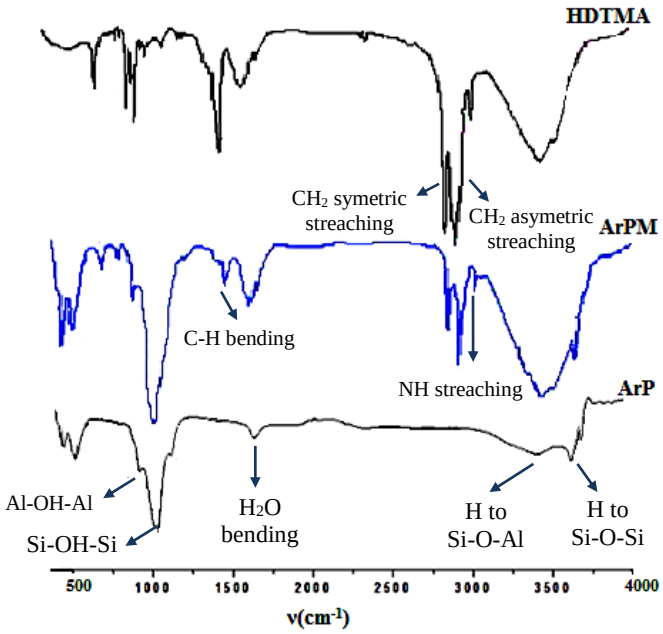

fig.5*: FT-IR Spectra of HDTMA molecule, ArP and ArPM*

III.1.4 XRD of organosmectite

The XRD patterns of ArP and ArPM were recorded in the range of 2 to 10° (2Θ) at a scanning speed of 1°min^{-1}(fig.6) using diffractometer with Cu Kα radiation.

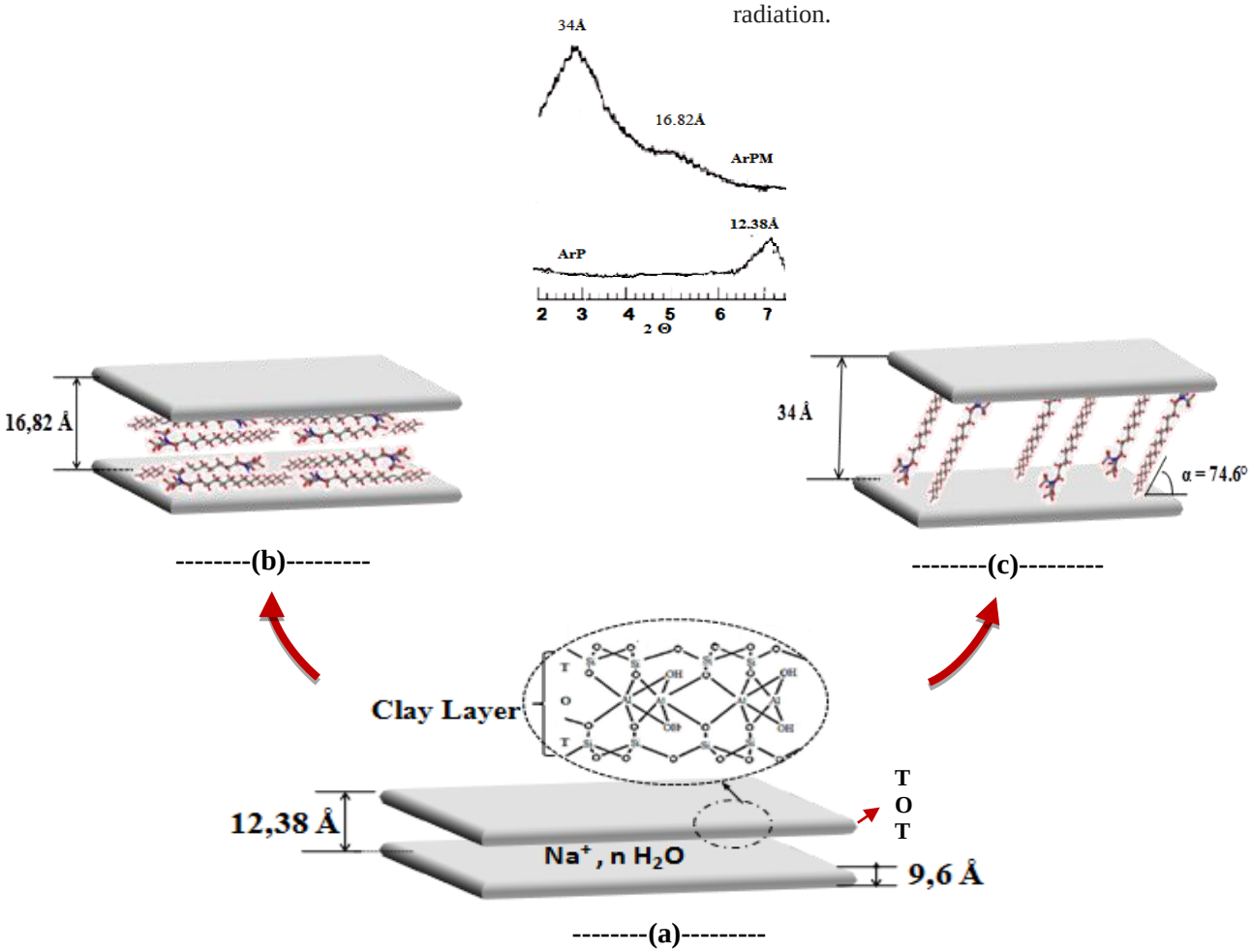

fig 6 *: XRD of ArP and ArPM*

(This work is licensed under a Creative Commons Attribution 4.0 International License.)

International Journal of Engineering Research & Technology (IJERT)
ISSN: 2278-0181
Vol. 5 Issue 02, February-2016

The basal diffraction peak, d_{001},of ArP emerges at 6.8(2Θ) with the distance of 12.38Å shifts to the higher values (34 Å) point out that the penetration of the surfactant cations into the interlayer space of bentonite occurs, sodium ions on the interlayer of the smectite are randomly or selectively replaced with HDTMA cations gives organophilic clays.

The values of d_{001} increase gradually (12.38Å →16.82 Å →34Å). The expansion in the basal spacing ($\Delta d=d_{001}$-9.6) varied from Δd=0.278nm for ArP to reach maximum Δd =2.44 nm for ArPM.

Expansions of bentonite layers are related to the arrangements of HDTMA molecules (fig6) [17-18].The arrangements of the surfactant molecules in the interlayer region of the smectite can be distinguished by comparing the interlayer expansions (Δd) and molecular dimension of the surfactant.

According to the data of van der Waals radius, covalent bond radius and bond angle, the steric configuration, size and shape of HDTMA organic cations could be calculated (fig.2) [19]. When the $HDTMA^+$ is lying flat, the height of alkyl-chain is 4.1Å and the 'nailhead' is 5.1Å.

accordingly peak at 16.82Å (d_{002}) hold an interlayer space of ~0.722nm, in the ArPM hybrid sample, suggest lateral bilayer of organic ion arrangement, since the height of the lateral bilayer is 0.81 nm [20]; Lateral bilayer (LB) is that the protruding methyl inserts into cavity between organic cations or into the hexagonal hole of basal oxygen plane [21], consequently, the alkyl chains may come close together and arrange in lateral bilayer model (fig6 (b)). In view of that, the height of LB model depends on the height of the double layers of alkyl chains rather than that of cation end of $HDTMA^+$.

Reflection at 34Å in ArPM relate to the (001) peaks suggesting an evolution of paraffin-type monolayer arrangement with a maximum interlayer expansion of 24.4 Å (fig6.c).

Angles, α, between the alkyl chain and basal surface was also estimated, taking into account the length of $HTDMA^+$ (25.3Å) and the height of TOT layer (9.6Å), α ≈74.6° for the paraffin monolayer arrangement (fig6.c).

Result suggests that interlayer cations in smectite should be replaced by $HDTMA^+$ entirely, since there is no basal spacing at ~ 12.38Å corresponding to ArP found in the XRD patterns of hybrid sample. Consequently, we recommend that there is no Na-smectite layer in the hybrid prepared in the range of 3CEC. Adsorption mechanism of the surfactant with the clay sheets can be estimated by the following graphic (fig.7).

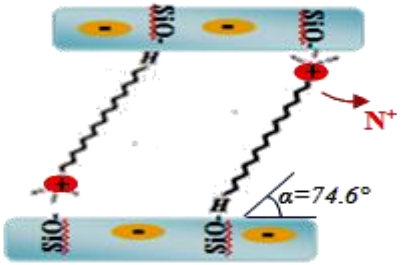

***fig7**. Adsorption mechanism of surfactant by clay layer*

III.1.5 Scanning electron microscope (SEM)

SEM photomicrographs obtained for Na-smectitet and organo sample are illustrated in fig. 8. Surface of ArP looks very smooth with fluffy appearance and curved plates. After cationic surfactant insertion reaction significant changes were observed. Surface morphology loses its foliated structure and became rougher with many small and aggregated particles and the plates become relatively flat, this is probably occurred due to the reduction in certain crystalline domains of the clay particles with the surfactant packing density in the interlayer, the curved plates in ArP will change to flat layers.

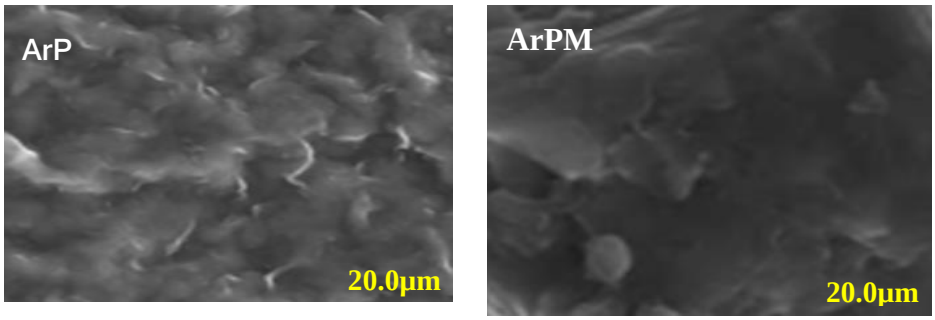

fig.8: SEM images of Na-Smectite and organosmectite

(This work is licensed under a Creative Commons Attribution 4.0 International License.)

International Journal of Engineering Research & Technology (IJERT)
ISSN: 2278-0181
Vol. 5 Issue 02, February-2016

III.1.6 X-ray photoelectron spectroscopy (XPS) characterization

XPS was a sensitive technique applied to probe the surface chemical composition and chemical states of the prepared organomaterial (ArPM) as a result of ion exchange reactions. Figure 9 shows the XPS survey scans of Na-Smectite (ArP), HDTMAB and representative organoclay ArPM.

The survey scan divulge the presence of sodium, silicon, aluminium, iron, and magnesium in the Na-Smectite, the XPS result is in excellent agreement with our chemical analysis result of Na-Smectite. It has also indentified the presence of carbon, nitrogen, and bromine in HDTMAB. In addition, there is a minor amount of oxygen in HDTMAB and carbon in ArP, resulting from adsorbed CO_2 [22].

Trace amount of magnesium and iron are seen in the scans of ArPM, whereas the sodium peak is disappeared. Both magnesium and iron are located in the ArP structure rather than in the interlayer. The absence of sodium ions in the ArPM confirms the sodium ions are exchanged when cationic surfactants are introduced in the interlayer this result corroborates with those of XRD.

In addition the Al/Si ratio dropped from 0.32 (ArP), this value is in good agreement with the chemical analysis of ArP (0.3), to 0.26 (ArPM). As the intercalation of surfactants increases in the interlayer, the distance between Al-O(OH) octahedral sheets and two Si-O tetrahedral sheets in the structure of ArP is expanded, and hence, the detecting ratio of Al and Si is lower.

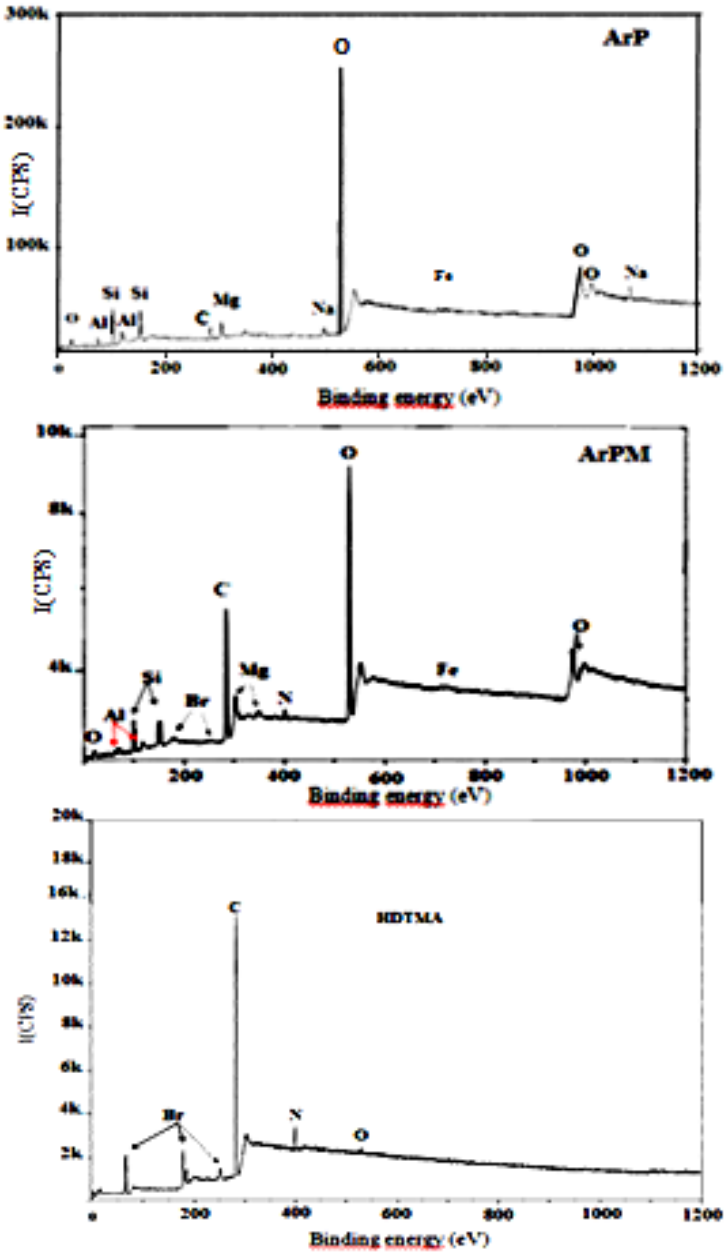

fig.9: XPS survey scans of HDTMAB, ArP and the representative ArPM

(This work is licensed under a Creative Commons Attribution 4.0 International License.)

International Journal of Engineering Research & Technology (IJERT)
ISSN: 2278-0181
Vol. 5 Issue 02, February-2016

III.1.7 Potentiometric titration

Surface charge density σ_H of the clay sample was determined by potentiometric acid–base titration using NaCl as background electrolyte at constant ionic strengths for different concentrations (0.5, 0.1 and 0.01M) to guess the effect of ionic strength on the surface charge density σ_H and to determine the pH were σ_H=0. This pH value is referred to the point of zero net proton charge, noted pH_{PZC}.

Titration curves were similar in shape for the range pH used (fig.10) and concord very well with previous works [23]. In the acidic pH range, the degree of protonation increased with increasing ionic strength and the opposite was observed in the alkaline pH range. The dependence of the surface charge density on the ionic strength was due to the fact that ionic strength had significant and contrasted effects on the dissolved species Al, Si, Fe and Mg [24]. ArPM has a surface charge density higher than ArP. This high surface charge density was produced by protonation and deprotonation of inner-sphere ArPM hydroxyl surface complex formed at variable-charge hydroxyl groups at the edges [23].

PZC of the organobentonite moved to the basic pH according to the $HDTMA^+$ intercalation (fig. 9) in comparaison with that of ArP. PZC increase from 6.6 (ArP) to ~9 (ArPM).

Modifications of Na-smectite by Surfactant have an important role in surface charge behavior of the adsorbent. The loading of surfactants causes a transformation of clay surface property from hydrophilic to hydrophobic. Hydrophobicity suppressed the formation of bound HO layers on the surface.

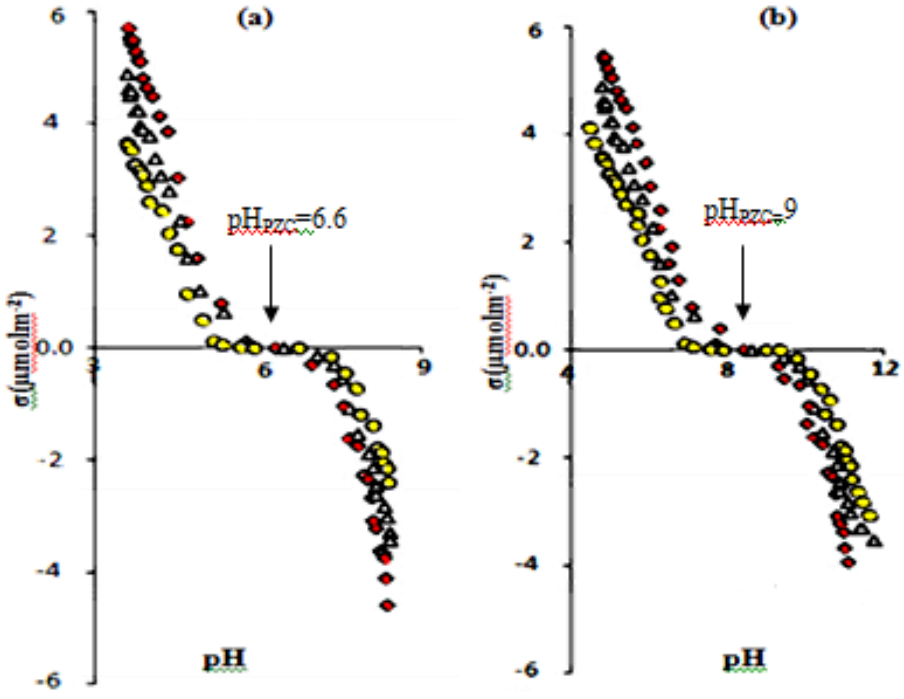

fig. 10: Potentiometric titration curves versus pH at different ionic strengths of (a) ArP anf (b) ArPM, at 279 K

◆ I=0.5 △ I=0.1 ○ I=0.01

III.1.8 Zeta potentiometric

The zeta potential of the ArP and ArPM were measured at various pH (Fig. 11). The purified smectite has a point of zero charge (p.z.c.) of 6.5, after modification by HDTMA surfactant at 3 CEC level the p.z.c. moved to 9.2, these values were in excellent agreement with those of potentiometric titration.

(This work is licensed under a Creative Commons Attribution 4.0 International License.)

International Journal of Engineering Research & Technology (IJERT)
ISSN: 2278-0181
Vol. 5 Issue 02, February-2016

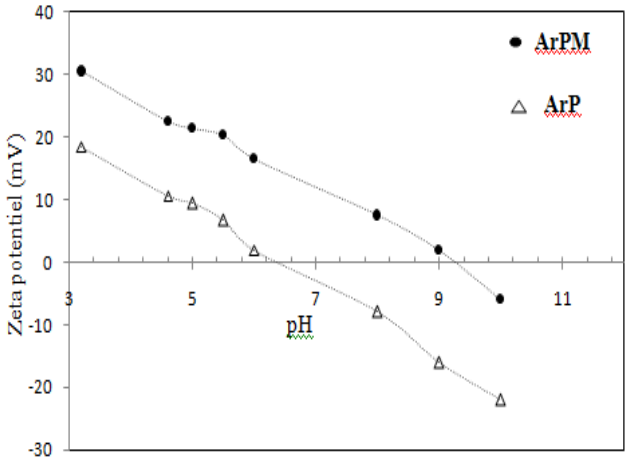

fig.11. Effect of pH on the zeta potential of ArP and ArPM.

III.1.9 Specific surface area S_{BET} and cation exchange capacity (CEC)

Specific surface area (figures not shown), pore volume, and CEC of the ArP and hybrid organoclay are presented in table 2.

Surface area drops dramatically from 110 cm^3g^{-1} (ArP) to 0.64cm^3g^{-1} (ArPM). It is also found that the pore volume decrease significantly. This is due to the fact that interparticle pores of smectite are covered and the interlamellar spaces are blocked, lead to inhibition of the passage of N_2 molecules. Micropores surface area (Sμp) and micropores volumes (Sμp) were annulled after the organophilic modification.

The cation exchange capacity (CEC) of ArP and the hybrid organoclay, estimated by using $Cu(EDA)_2^{2+}$and ammonium acetate methods, show the same magnitude. CEC decreases from 98.6 (ArP) to 6meq/100g (ArPM). These results confirm those of acid-base potentiometric titration. The PZC of ArPM was basic (table 2), adsorption of the surfactant modify the surface character. The increase of pH_{PZC} after surfactant treatment indicates that the organoclay becomes more positive and the surface properties of the adsorbent change from hydrophilic to hydrophobic by the substitution of Na^+ interlayer cation by $HDTMA^+$ cation. Oragnoclay generate higher adsorption capacity for anionic compound. Similar remarks were reported in many previous studies [20-21-25].

Table2. Textural parameters and CEC studied of ArP and ArPM and pH_{PZC}

samples	S_{BET}	$S_{\mu p}$	V_p	$V_{\mu p}$	CEC (meq/100g)	CEC (meq/100g)	pH_{PZC}	
	(m^2g^{-1})		(cm^3g^{-1})		Ammonium acetate method	$Cu(EDA)_2^{2+}$ method	Potentiometric	Zeta metric
ArP	110	8.7	0.138	0.016	98.6	97.56	6.6	6.5
ArPM	0.63	-	0.001	-	6	8	9	9.2

From XRD, CEC and S_{BET} results it can be estimative that $HDTMA^+$ occupies interlayer space, via cation exchange with Na^+ interlayer and surface adsorption sites. This can well explain the dramatic surface area and pore volume decrease of organoclay compared to those of starting clay.

IV ADSORPTION STUDIES

IV.1 Sorption isotherms

Adsorption isotherms were determined at 25°C by shaking 100mg of the adsorbent (ArP) with 50ml of CR solution with variant concentrations for 60min at natural pH (pH=6.2). After shaking at 5000tr/min, the solution was separated from the solid by centrifugation. The residual concentrations in the supernatants were determined by UV-visible spectrophotometer at 498 nm, and the solid phases were analyzed by FTIR spectroscopy at the range 400 to 4000nm^{-1}.

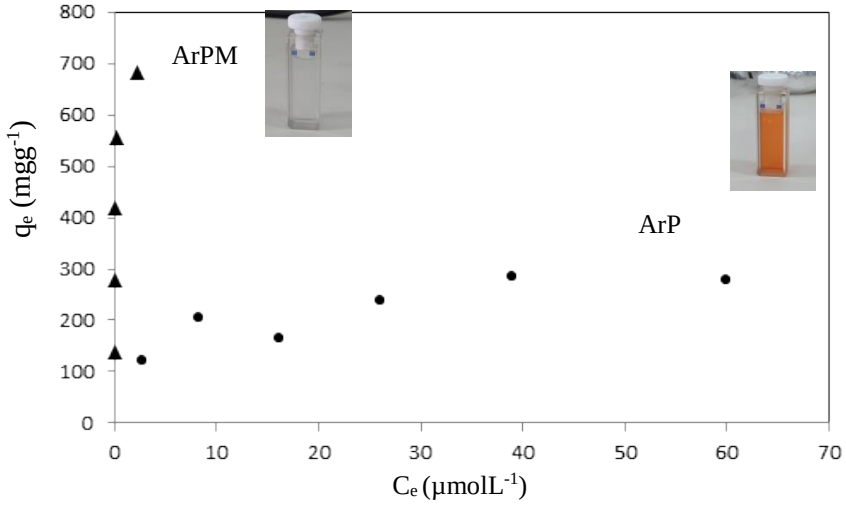

fig.12: Adsorption isotherm of CR by ArP and ArPM

(This work is licensed under a Creative Commons Attribution 4.0 International License.)

International Journal of Engineering Research & Technology (IJERT)
ISSN: 2278-0181
Vol. 5 Issue 02, February-2016

Adsorption isotherms of congo red by ArP (fig.12), expressing the adsorbed amounts (q_e) as a function of equilibrium concentration (C_e), is L-type [26]. In this kind of isotherm, the initial portion provides information about the availability of the active sites to the adsorbate and the plateau suggests a monolayer formation. The initial curvature indicates that a large amount of dye is adsorbed at a lower concentration as more active sites of ArP are available. As the concentration increases, it becomes difficult for a dye molecule to find vacant sites, and so monolayer formation occurs.

Adsorption of CR takes place possibly by means of surface exchange reactions until the surface functional sites are completely full, thereafter dye molecules diffuse into the smectite layers for further interactions and/or reactions such as ion-exchange, complexation interactions [27-28]. This reaction mechanism may be partly due to complexation between the negatively charged groups (D–SO_3^-) in CR and positively charged Al_2O_3 groups on the smectite surface or to ion exchange between positively charged groups (D–$^+NH_3$ or –$^+$NH=N–) in CR (fig.13) and Na^+ ions, initially present in the exchange position of the smectite.

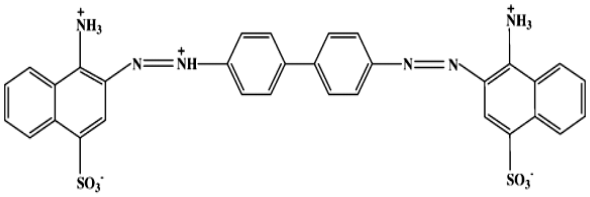

Fig.13: Protonated Congo red — ammonium rich variety at natural pH

According to previous work the hydrolysis of Si–OH or Al–OH bonds along the clay lattices produces the surface charge. Depending on the silica structure and the pH of the solution, the net surface charge can be either positive or negative. Adsorption of cations was favoured at pH > pH_{PZC}, while the adsorption of anions was favoured at pH < pH_{PZC}.

In the aqueous solution, the acid dye is first dissolved and the sulfonate groups of the acid dye (D–SO_3Na) are dissociated and converted to anionic dye ions at natural solution pH of 6.2. The pH_{PZC} of ArP was 6.5 at this condition Arp develop more positive charge witch explain the amout of dye removal. Adsorption mecanism can be estimated and reprisented by figure.14.

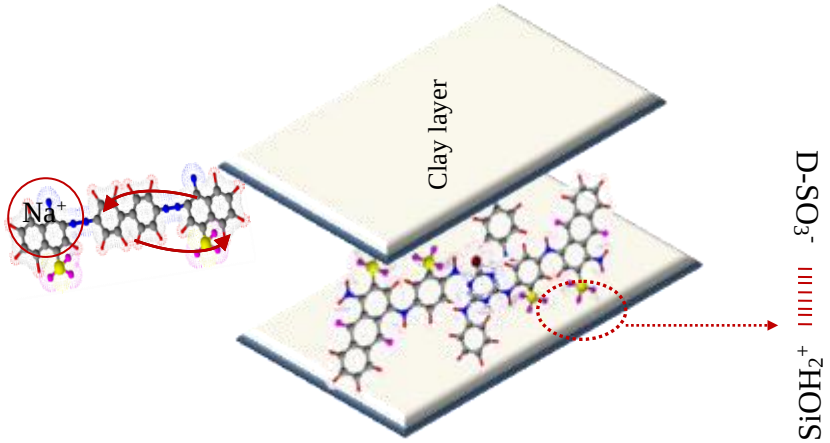

fig.14 : CR adsorption mechanism

Uptake of CR by ArP has been confirmed by FTIR study (fig. 15). Results show a news absorption bands in ArP FTIR spectrum after dye adsorption, in comparaison with FTIR spectrums of ArP and CR, these bands linked to specific functionals groups of CR structure (table 3).

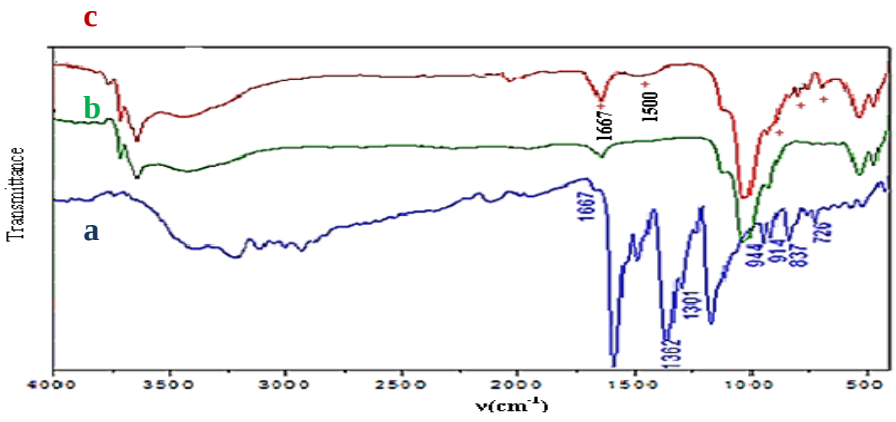

***Fig 15**: FTIR spectrums of: **(a)** CR powder only, **(b)** ArP befor CR adsorption and **(c)** ArP after CR adsorption*

(This work is licensed under a Creative Commons Attribution 4.0 International License.)

International Journal of Engineering Research & Technology (IJERT)
ISSN: 2278-0181
Vol. 5 Issue 02, February-2016

Table 3: Most important adsorption bandes of CR functional groups

Functional groups	$\upsilon(C=C)_{Ar}$	$\upsilon(N-H)$	$\delta(C-H)_{Ar}$
Frequency (cm^{-1})	*1667*	*1500*	*837-914 -726*

IV.2 Effect of pH on dye removal

From our previous study and other works in the literature dye adsorption is strongly dependent on pH solution. This can be attributed to the chemical form of dye in solution and functional groups present on the adsorbent surface at a specific pH. CR is a diazo anionic dye and is a pH sensitive, exposure to HCl causes color change from red to blue, due to π–π* transition of azo group shift to higher wavelength because of protonation [29]. At lower pH CR become cationic and shows two tautomeric form [30], i.e. ammonium rich variety and azonium variety (fig.16).

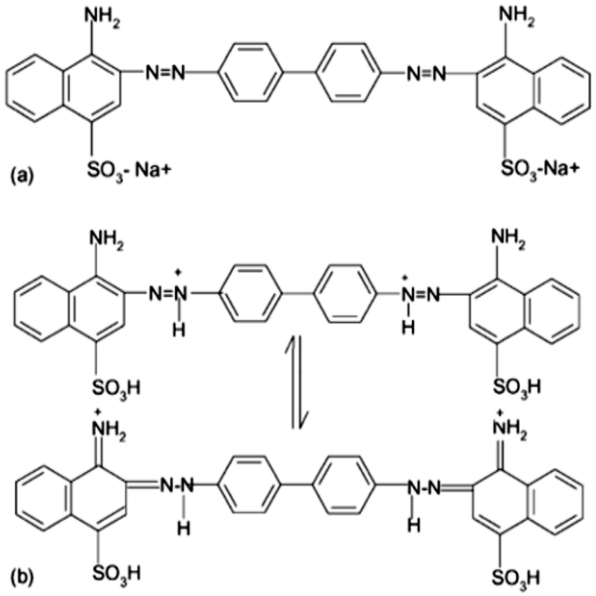

Fig16: Protonated Congo Red at (a) pH>5.5, (b) pH<5.5[29-3(

In this work, effect of initial pH of dye solution on the amount of adsorbed dye was studied at 25°C over a range of pH from 2 to 12. Experiments were conducted on suspensions of 0.1g of ArP in 50ml of dye solution with initial concentration of 69.66mgL^{-1}. The suspensions were stirred for 1h and then centrifuged. Dye concentrations in the supernatant were measured by UV-visible spectrophotometer at appropriate λ_{max} [30]. The pH was adjusted by adding a few drops of NaOH or HCl before each experiment.

The amount of dye adsorbed per unit mass of adsorbent at equilibrium as shown in figure 17 increased as pH was increased from 2 to 5, reaching a maximum at pH range 4-5 with adsorption efficiency and 92% of dye removal. We have noted an almost complete discoloration of the solution for pH range 5 to 6. The maximum adsorption can be stimated at pH = 5.7.

At lower pH the negatively charged silica sites of bentonite are neutralized by H^+ ions and alumina sites are positives, the number of negatively surface charged decrease, However significant CR adsorption was reached. In another hand, at lower pH CR (dipolar molecule H_3N^+-R-SO_3^-) present tow protonated tautomeric species (fig 16b): an ammonium form, where the protons attached to the amino nitrogen and an azonium form, they were attached to the α-azo nitrogen. Many functional N-sites are present on CR and some of nitrogen form hydrogen bonds by accepting protons from the solution and some are protonated to form cationic species.

.

Therefore the maximum adsorption of cationic dye at lower pH may be due to the mechanism of cation exchange, replacing Na^+, initially present in the interlayer space of bentonite. Thereafter, adsorption decreased with increasing pH. Above pH 6, the percentage of dye removal drops. The overhead setup can be attributed to the changes in the polarity of the electric double layer on both the silica and alumina contents of the clay from positive to negative. The high negatively charged adsorbent surface sites (at high pH) did not favor the adsorption of deprotonated CR due to electrostatic repulsion. Also, an abundance of OH^- ions in basic solution creates a competitive environment with anionic ions of CR for the adsorption sites causing a significant reduction in the removal of CR dye from the solution.

It can be suggested that $–NH_2$, -N=N-, -HN-N and SO_3^- groups of CR were involved in the adsorption

(This work is licensed under a Creative Commons Attribution 4.0 International License.)

International Journal of Engineering Research & Technology (IJERT)
ISSN: 2278-0181
Vol. 5 Issue 02, February-2016

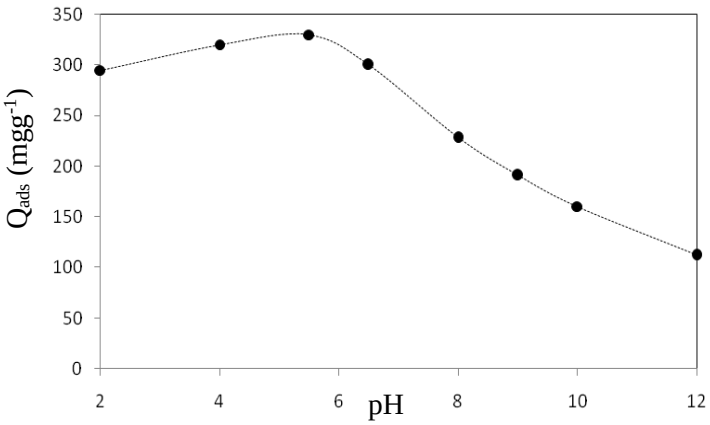

fig 17: Effect of pH on CR removal by ArP

IV.3 Modelization of experimentals data

Equilibrium data of Congo red adsorption on purified bentonite (ArP) were analyzed using the linearized form of Freundlich and Langmuir models.

(i)- *The Langmuir isotherm* [31] assumes monolayer adsorption on a uniform surface with a finite number of adsorption sites. Once a site is occupied, no further sorption can take place at that site, the surface will eventually reach a saturation point where the maximum adsorption of the surface will be achieved. The linear form of the Langmuir isotherm model (Eq1) is given in table 5.

Accordingly experimental adsorption data were analyzed using the linearized form of Langmiur isotherm, obtained by plotting $\frac{C_e}{q_e}$ versus C_e (fig18). The calculated Langmuir isotherm constants and the corresponding coefficient of correlation, R^2 are shown in table 4.

(ii)- *The Freundlich model*: is applicable to monolayer (chemisorption) and multilayer adsorption (physisorption) and is based on the assumption that the adsorbate adsorbs onto the heterogeneous surface of an adsorbent [32]. The linear form of Freundlich equation (Eq2) is given in table 4.

The equilibrium data were further analyzed using the linearized form of Freundlich isotherm, by plotting $\ln q_e$ versus $\ln C_e$ (fig19). The calculated Freundlich isotherm constants (K_F ,n) and the corresponding coefficient of correlation, R^2 are shown in table 5.

Table.5: Langmuir and Freundlich parameters

Langmiur model				*Freundlich model*		
Linearized eqations						
$\frac{C_e}{q_e} = \frac{1}{k_L} q_m + \frac{C_e}{q_m}$ (Eq1)				$\ln q_e = \frac{1}{n} \ln C_e + \ln K_F$ (Eq2)		
q_m: maximum adsorption capacity (mgg^{-1})		K_L Langmuir constant (Lmg^{-1})	C_e :equilibrium concentration (mgL^{-1})		n: adsorption intencity	K_F:Freundlich constant (Lmg^{-1})
R^2	R_L	K_L	q_m	R^2	1/n	K_F
0.979	0.026	0.537	372.13	0.892	0.406	387.22

As can be noted from modelization results, experimentals data concord very well with Langmuir model (R^2= 0.979), in an other hand the value of maximum adsorption capacity, q_m, determined from Langmuir plot close estimately more than the half of the experimental value. Hence it can be deduced that CR adsorption phenomena in ArP sample, wtitout any further modefication, is a monolayer adsorption mecanisme with a good rate of removal.

Essential characteristics of Langmuir isotherm can be expressed in terms of a dimensionless constant separation factor R_L that is given by the following equation (Eq5) :

$R_L = 1/ (1+ K_L C_0)$ where C_0 (mgL^{-1}) is the initial concentration of adsorbate, and K_L is Langmuir constant. The value of $R_L$indicates the shape of the isotherm which is [33]: (i) unfavorable ($R_L > 1$), (ii) linear ($R_L = 1$), (iii) favorable ($0 < R_L < 1$), (iv) or irreversible ($R_L = 0$). The R_L values are observed to be in the range 0–1(table 5), indicating that the adsorption was a favorable process.

IV.5 Adsorption of CR by ArPM

The same conditions of CR adsorption experiment by ArPM as the adsorption of this dye by ArP was used to test the performance of this

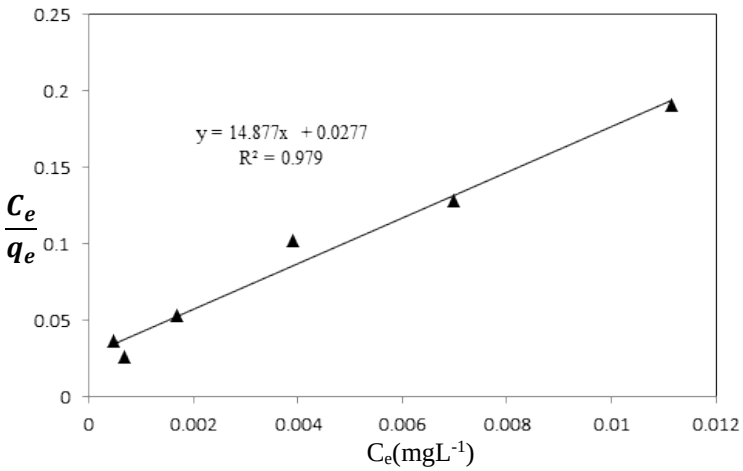

fig14*: Lngmuir plots of CR by ArP*

(This work is licensed under a Creative Commons Attribution 4.0 International License.)

International Journal of Engineering Research & Technology (IJERT)
ISSN: 2278-0181
Vol. 5 Issue 02, February-2016

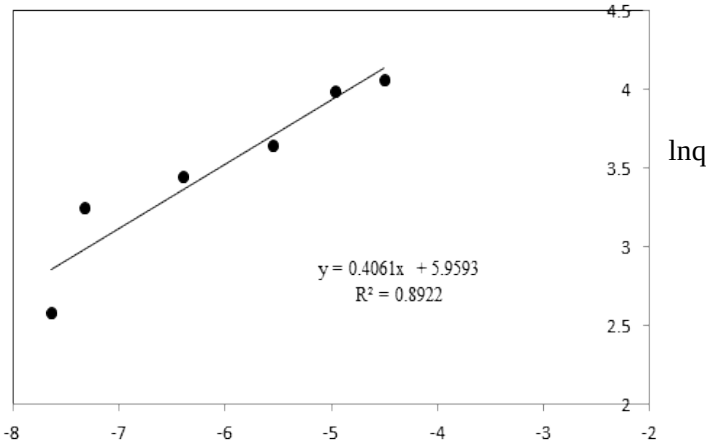

***fig15**: Freundlichplots of CR by ArP*

low cost nanoadsorbent for anionic dye removal (fig.8).
Adsorption of CR at natural pH=6.2 onto HDTMA-smectite (ArPM) is greater than the amount retained by ArP (fig.9), it represent two time the amount of CR removal by ArP. This can be explained by the hydrophobic character, the greater interlayer expansion and the high positive charge surface that developed this adsorbent. pH_{pzc} (9.2) and Δd_{001} (24.4Å) of ArPM facilities CR diffusion into interlayer space. The higher adsorption capacity of the dye onto ArPM was estimated due to the electrostatic attraction between the negatively charged $-SO_3^-$ of anion dye and interaction between the cationic surfactant head groups ($-N^+(CH_3)_3$). The maximum adsorption reach ~100% and total discoloration was noted.
When ArPM was saturated with HDTMAB, the specific surface area was only $0.63 m^2 g^{-1}$. However, the adsorption capacity of CR is as high. Congo red molecules were adsorbed into the interlamellar, this information was confirmed by XRD since the d_{001} of ArPM after CR adsorption increased from 34Å to 45 Å (figure not presented).

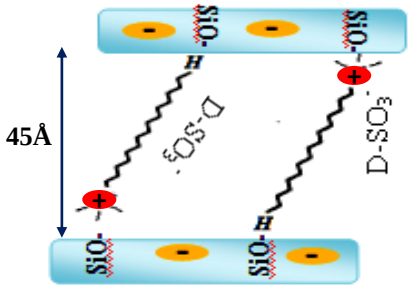

***fig.9** : Estimation mechanism of CR sorption by ArPM*

As reported by Fu [34] the two primary amines ($-NH_2$) attached to the two naphthalene rings located at the two ends of the CR molecule can be protonated ($-NH_3$) at the initial pH of 6 and could have stronger basicity, which could result in the attraction between the protonated amine ($-NH_3$) and the negatively charged surface (SiO_2 sites) of the adsorbent. They also proposed that electrostatic attraction was the primary mechanism, while other mechanisms could also be involved in the biosorption of CR.

V. CONCLUSION

Adsorption results reveals that the locally collected bentonite, without any further modification, can be used as adsorbent to remove anionic organic compound from wastewater, the ratio of CR removal by ArP achieve 58% with 0.1g, since it develop a remarkable positive charge density compared to other low cost adsorbent, further more organosmectite appear very important for this approach, employed as adsorbent for CR removal from aqueous water it give total discoloration for the dye solution (98.7% of dye removal), the amount of dye removal close approximately to initial dye concentration used.

Adsorption data of ArP concord very well with Langmuir model (R^2= 0.979), in an other hand the value of maximum adsorption capacity, q_m, determined from Langmuir plot close to more than a half of the experimental value. Hence it can be deduced that CR adsorption phenomena in ArP sample, wtitout any further modefication, is a monolayer adsorption mecanisme with a good rate of removal. Chimisorption processe was figured out for CR removal. From our point of view ArP can be used without modification yet we use more amount of adsorbent ArP) to reach 100% of CR remonal.

REFERENCES

[1] N. Kannann and M. Sundaram, Kinetics and mechanism of removel of méthyllene blue by adsorption on various carbons-a comparatives study. Dyes and Pigments ; 51 (2001) 25-44.
[2] H. Zollinger, Synthese properties and applications of organic dyes and pigments.Color chemistry, VCH. (1987).
[3] L.Rehn**.** Blasengeschwulste bei Fuschin arbeiten. Arch. KlinChir; 50 (1895) 588.
[4] M.K. Purkait, A.Maiti, S. DasGupta, S. De. Removal of congo red using activated carbon and its regeneration, J. Hazard. Mater. 145 (2007) 289–295.
[5] I.L. Finar. Organic Chemistry The Fundamental Principles, 1, sixth ed., Addison. Wesley Longman Ltd., England, 1986.
[6] A.S. Özcan, A. Özcan, Adsorption of acid dyesfrom aqueous solutions onto acid activated bentonite. J. Colloid Interface Sci. 276 (2004) 39–46.
[7] I. Mantin, Mesure de la capacité d'échange cationique des minéraux argileux par l'éthylène diamine et les ions complexes de l'éthylène diamine. C.R. Sci. Paris ; 269 (1969) 815–818.
[8] F. Bergaya, M. Vayer, CEC of clay Measurement by adsorption of a copper éthylènediamine complexem.Appl. Clay. Sci; 12 (1997) 275–280.
[9] F. Ayari, E. Srasra and M. T. Ayadi, Characterization of bentonitic clays and their use as adsorbent. Desalination; 185 (2005) 391– 397.
[10] I. Jarraya, S. Fourmentin, M. Benzina, S. Bouaziz. J. Chem. Eng; 89 (2011) 392–400.
[11] M. Sakizci, B. Alver, E. Yorukogullari. E. Therm. J. Anal. Calorim; 98 (2009) 429–436.
[12] Madejova´ J. (2003) FT-IR techniques in clay mineralstudies. Vibrational Spectroscopy, 31, 1-10.
[13] Madejova´ J., Komadel P. &Cicel B. (1994) Infraredstudy of octahedral site populations in smectites.Clay Minerals, 29, 319-326.
[14] Silverstein R.M. & Webster F.X. (1998) Spectrometric.Identification of Organic Compounds, 6th edition,John Wiley, New York.
[15] Li, Z.,Gallus, L., 2005. Surface configuration of sorbedhexadecyltrimethyl ammonium on kaolinite as indicated by surfactant and counterion, sorption cation desorption and FTIR. Colloids Surf. A 264, 61–67.
[16] Xi, Y., R.L. Frost, H. He, T. Kloprogge, Wyoming Montmorillonite Surfaces Using a Cationic Surfactant.Langmuir, 2005. 21(19): p. 8675-8680.

(This work is licensed under a Creative Commons Attribution 4.0 International License.)

International Journal of Engineering Research & Technology (IJERT)
ISSN: 2278-0181
Vol. 5 Issue 02, February-2016

[17] V Ponnusami; R Aravindhan; N Karthik Raj; G Ramadoss; SN Srivastava, J. Environ. Prot. Sci., 2009, 3, 1–10.
[18] S Liang; X Guo; N Feng; Q Tian, J. Hazard. Mater., 2010, 174(1-3), 756–762.
[19] Zhou, G. D., Inorganic Structural Chemistry (in Chinese), Beijing: Science Press, 1984, 118-119.
[20] Lagaly, G., Layer charge heterogeneity in vermiculites, Clays and Clay Minerals, 1982; 30: 215-222.
[21] Faridi, A. v., 15. Guggenheim, S., Crystal structure of tetramethylammonium-exchanged vermiculite, Clays and Clay Minerals, 1997,45: 859-866.
[22] Bugyi, L.; Oszkó, A.; Solymosi, F. Surf. Sci. 2000, 461, 177-190.
[23] F. Huertas, L. Chou, R. Wollaster, Mechanism of kaolinite dissolution at room temperature and pressure: Part I. Surface speciation. Geochimica et Cosmochimica Acta 62(1998) 417–431.
[24] M. Duc, F. Gaboriaud, F. Thomas, Sensitivity of the acid–base properties of clays to the methods of preparation and measurement 2. Evidence from continuous potentiometric titrations. Journal of Colloid and Interface Science 289 (2005) 148–156.
[25] Z. Li, W.T. Jiang, H. Hong, Spectrochimica Acta Part A: Molecular and Biomolecular Spectroscopy 71 (2008) 1525.
[26] C.H. Giles, T.H. Mac Ewan, S.N. Nakhwa, D. Smith, Studies in adsorption. Part XI. A system of classification of solution adsorption isotherms, J. Chem. Soc; 4 (1960) 3973–3993.
[27] M. ¨ Ozacar, ˙ I.A. S ¸ engil, A two stage batch adsorber design for methylene blue removal to minimize contact time, J. Environ. Manage. 80 (2006)372–379.
[28] G. Crini,H.N. Peindy, F.Gimbert, C. Robert, Removal of C.I. basic green 4,(malachite green) fromaqueous solutions by adsorption using cyclodextrin-based adsorbent: kinetic and equilibrium studies, Sep. Purif. Technol. 53(2007) 97–110.
[29] B. Onida, L. Flora, C.O. Arean, E. Garrone, Permeability of micelles of surfactant containing MCM-41 silica as monitored by embedded dye molecule, Chem. Commun; (2001) 2216–2217, doi:10.1039/b105261f.
[30] Z. Yermiyahu, I. Lapides, S. Yariv, Visible adsorption spectroscopy study of the adsorption of congo red by montormorillonite, ClayMiner; 38 (2003) 483–500.
[31] I. Langmuir, The Adsorption of Gases on Plane Surfaces of Glass Mica and Platinum., Journal of the American Chemical Society; 40 (1918) 1361-1403.
[32] H.M.F. Freundlich, Uber Die Adsorption in Losungen. Zeitschriftfur Physikalische Chemie; 57 (1906) 385-470.
[33] F. Ayari, E. Srasra and M. T. Ayadi, Retention of lead from an aqueous solution by use of bentonite as adsorbent for reducing leaching from industrial effluents, Journal of Dessalination; 206 (2007)240-278.
[34] Y. Fu, T. Viraraghavan, Dye biosorption sites in Aspergillus niger, Bioresour. Technol. 82 (2002) 139–145.

(This work is licensed under a Creative Commons Attribution 4.0 International License.)